

Transient electromagnetically induced transparency spectroscopy of ^{87}Rb atoms in buffer gas

Zi-Shan Xu(徐子珊), Han-Mu Wang(王汉睦), Zeng-Li Ba(巴曾立), and Hong-Ping Liu(刘红平)

Citation: Chin. Phys. B, 2022, 31 (**7**): 073201. DOI: 10.1088/1674-1056/ac4748
Journal homepage: http://cpb.iphy.ac.cn; http://iopscience.iop.org/cpb

What follows is a list of articles you may be interested in

Light-shift induced by two unbalanced spontaneous decay rates in EIT (CPT) spectroscopies under Ramsey pulse excitation

Xiaoyan Liu(刘晓艳), Xu Zhao(赵旭), Jianfang Sun(孙剑芳), Zhen Xu(徐震), and Zhengfeng Hu(胡正峰)
Chin. Phys. B, 2021, 30 (**8**): 083203. DOI: 10.1088/1674-1056/ac0528

Precise measurement of a weak radio frequency electric field using a resonant atomic probe

Liping Hao(郝丽萍), Yongmei Xue(薛咏梅), Jiabei Fan(樊佳蓓), Jingxu Bai(白景旭), Yuechun Jiao(焦月春), Jianming Zhao(赵建明)
Chin. Phys. B, 2020, 29 (**3**): 033201. DOI: 10.1088/1674-1056/ab6c49

Rydberg electromagnetically induced transparency and Autler-Townes splitting in a weak radio-frequency electric field

Liping Hao(郝丽萍), Yongmei Xue(薛咏梅), Jiabei Fan(樊佳蓓), Yuechun Jiao(焦月春), Jianming Zhao(赵建明), Suotang Jia(贾锁堂)
Chin. Phys. B, 2019, 28 (**5**): 053202. DOI: 10.1088/1674-1056/28/5/053202

Vapor cell geometry effect on Rydberg atom-based microwave electric field measurement

Linjie Zhang(张临杰), Jiasheng Liu(刘家晟), Yue Jia(贾玥), Hao Zhang(张好), Zhenfei Song(宋振飞), Suotang Jia(贾锁堂)
Chin. Phys. B, 2018, 27 (**3**): 033201. DOI: 10.1088/1674-1056/27/3/033201

Laser frequency locking based on Rydberg electromagnetically induced transparency

Yuechun Jiao(焦月春), Jingkui Li(李敬奎), Limei Wang(王丽梅), Hao Zhang(张好), Linjie Zhang(张临杰), Jianming Zhao(赵建明), Suotang Jia(贾锁堂)
Chin. Phys. B, 2016, 25 (**5**): 053201. DOI: 10.1088/1674-1056/25/5/053201

Transient electromagnetically induced transparency spectroscopy of ^{87}Rb atoms in buffer gas

Zi-Shan Xu(徐子珊)[1,2], Han-Mu Wang(王汉睦)[1,2], Zeng-Li Ba(巴曾立)[3], and Hong-Ping Liu(刘红平)[1,2,†]

[1] *State Key Laboratory of Magnetic Resonance and Atomic and Molecular Physics, Wuhan Institute of Physics and Mathematics, Innovation Academy for Precision Measurement Science and Technology, Chinese Academy of Sciences, Wuhan* 430071, *China*
[2] *University of Chinese Academy of Sciences, Beijing* 100049, *China*
[3] *School of Physical Science, University of Science and Technology of China, Hefei* 230026, *China*

(Received 16 October 2021; revised manuscript received 24 December 2021; accepted manuscript online 31 December 2021)

We study the transient response dynamics of ^{87}Rb atomic vapor buffered in 8 torr Ne gas through an electromagnetically induced transparency configured in Λ-scheme. Experimentally, the temporal transmission spectra versus probe detuning by switching on and off the coupling one show complex structures. The transmitted probe light intensity drops to a minimum value when the coupling light turns off, showing a strong absorption. Even at the moment of turning on the coupling light at a subsequent delayed time, the atomic medium shows a fast transient response. To account for the transient switching feature, in the time-dependent optical Bloch equation, we must take the transverse relaxation dephasing process of atomic vapor into account, as well as the fluorescence relaxation along with the optical absorption. This work supplies a technique to quantify the transverse relaxation time scale and to sensitively monitor its variation along the environment by observing the transient dynamics of coherent medium, which is helpful in characterizing the coherent feature of the atomic medium.

Keywords: electromagnetically induced transparency, rubidium atom, transverse relaxation rate

PACS: 32.70.Cs, 42.50.Gy, 32.80.Qk, 32.10.Fn **DOI:** 10.1088/1674-1056/ac4748

1. Introduction

A long spin polarization lifetime is an important issue for applications of alkali-metal vapor cells in atomic clocks,[1] quantum memory,[2] spin squeezing,[3] quantum optics,[4] and atomic magnetometers.[5] Spin diffusion, spin-destruction collisions and spin-exchange collisions are the main mechanisms which relax the spin of alkali atoms. Two conventional ways are widely used to suppress the spin-diffusion relaxation of alkali atoms. One method is coating the cell with an anti-relaxation coating, which decreases the depolarization rate of the alkali atoms due to collisions with the vapor cell wall.[6,7] The second method is adding buffer gas in vapor cell, generally noble gas. Buffer gases help the alkali atoms diffuse slowly to the wall, so they preserve long spin polarization by decreasing the wall collision rate.[8] This application requires the highly non-equilibrium polarizations of the noble gas nuclei to be long lived. The spin polarization of the alkali-metal atoms is very sensitive not only to the power of the pumping and probe light, but also to the cell temperature and wall conditions, therefore it is important to find a convenient method to measure and monitor the transverse spin relaxation time of alkali-metal atoms.

Various methods have been used to measure the transverse relaxation mechanism of alkali-metal atoms. Kominis *et al*. deduced the transverse spin relaxation rate by observing the width of the power spectrum of the Faraday rotation angle fluctuations induced by spin noise on the polarization of the probe laser.[9] Another method is the pump and probe scheme in which the alkali-metal atom spins were optically pumped by circularly polarized light and the spin precession was monitored via optical rotation of linearly polarized probe light oriented perpendicular to the pump beam direction.[10] Liu *et al*. experimentally measured the spin relaxation of the alkali-metal atoms in a cell by detecting the frequency shifts due to the spin-exchange interaction.[11] The spin relaxation effect of the magnetic-field gradient has also been discussed and the transverse spin relaxation time is determined by using the magnetic resonance linewidths.[12] Recently the time-domain Franzen and Ramsey measurements have been used to produce high-resolution images caused by the transverse relaxation time in the Rb cell using a microwave cavity.[13]

The measurement of the spectral broadening and frequency shift is a feasible way to obtain the relaxation rate but it is difficult to sensitively monitor its tiny variation along environment. Instead, in this paper, we present a characterization technique to acquire the Zeeman transverse relaxation rate of ^{87}Rb with buffer gas by measuring the transient transmission spectrum of probe light of Λ-scheme EIT among ground state $5S_{1/2}$ Zeeman sublevels by turning on or off the coupling light. This technique has been applied to reveal many transient properties such as the precursor of optical pulse propagation in a dispersive medium[14–17] and switching effects.[18,19] Since the Zeeman transverse decay process is closely correlated with

†Corresponding author. E-mail: liuhongping@wipm.ac.cn
© 2022 Chinese Physical Society and IOP Publishing Ltd

the characteristic dynamics, we can evaluate its contribution unambiguously with the aid of the optical Bloch equation.

2. Theoretical model and experimental setup

We choose the coupling and probe lasers resonant to the transition $5S_{1/2}, F = 2 \rightarrow 5P_{1/2}, F' = 2$ of ^{87}Rb D_1 line. The concerned Λ-type EIT Zeeman splitting energy levels are shown in Fig. 1.

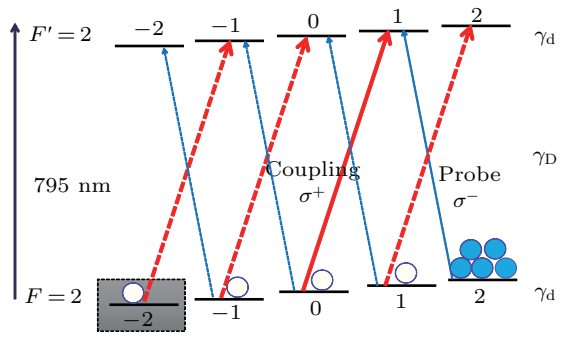


Fig. 1. Optical transitions of Λ-type EIT system among the Zeeman sublevels when the circularly polarized coupling and probe lasers are tuned resonant to transition $F = 2 \rightarrow F' = 2$ of ^{87}Rb D_1 line. The parameters γ_d and γ_D describe the relaxation processes between the Zeeman levels within the same hyperfine manifold F and between the upper and lower hyperfine levels, respectively.

As we know, the spin polarization of alkali-metal atoms in an optical system can be described by the time-dependent optical Bloch equation[20–22]

$$\frac{\mathrm{d}\rho(t)}{\mathrm{d}t} = -\frac{\mathrm{i}}{\hbar}[H(t), \rho(t)] + L\rho(t), \tag{1}$$

where $\rho(t)$ is the density matrix in interaction picture, and $H(t)$ is the Hamiltonian. Longitudinal and transverse relaxations must be included in L for a full description of the dynamics of atom. We can also extract all the interaction terms in L back to a complex Hamiltonian with dimension of 10, where 5 belongs to the upper Zeeman states and 5 to the lower Zeeman states. It has a form

$$\begin{bmatrix} \cdots & & & & \\ & \Delta_i - \frac{\mathrm{i}}{2}\gamma_i & & V_{ij} & \\ & & \cdots & & \\ & V_{ij}^* & & \Delta_j - \frac{\mathrm{i}}{2}\gamma_j & \\ & & & & \cdots \end{bmatrix}, \tag{2}$$

where Δ_i is the optical detuning of laser, γ_i is the relaxation rate corresponding to the natural lifetime, and V_{ij} stands for the interaction between two different state i, j. Its form depends on the two concerned states. If the two states are within the same upper or lower manifold, V_{ij} has a form $V_{ij} = -\frac{\mathrm{i}}{2}\gamma_d$, characterizing the transverse relaxation due to the interaction between neighbor Zeeman sub-levels, for example, in an angular momentum polarization of alkali-metal atoms in the Zeeman EIT Λ-system.[23,24] If the two states are attributed to the upper and lower states separately, $V_{ij} = \frac{\Omega_{c,p}}{2} - \frac{\mathrm{i}}{2}\gamma_D$, where the first term stands for the coupling induced by the laser applied following the transition selection rule and the second term indicates the relaxation induced by longitudinal phase loss during fluorescence. The laser-atom coupling is characterized by Rabi frequency $\Omega_{c,p}$ and the subscripts c,p takes c for the coupling beam and p for the probe beam, respectively. For simplicity, the transverse relaxation dynamics are described by the same parameter γ_d between the upper Zeeman levels and between the lower Zeeman levels. The parameter symbols are also indicated in Fig. 1 for better view of the their corresponding processes. If we apply a switching laser pulse for the atomic system, its transient dynamics will be described by the above time-dependent Eq. (1). Note that only the diagonal imaginary part follows the operation of classical brackets.

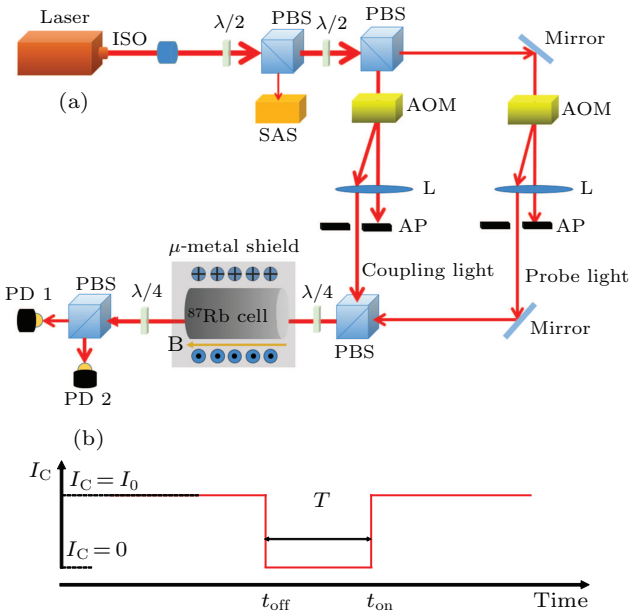


Fig. 2. (a) Scheme of the experimental setup. ISO: optical isolator; $\lambda/2$: half-wave plate; $\lambda/4$: quarter-wave plate; PBS: polarization beam splitter; SAS: saturated absorption spectroscopy; AOM: acousto-optical modulator; L: lens; AP: aperture slot; PD: photo detector. (b) The corresponding optical switch in time sequence for the coupling light, where the switching-off duration time T is taken as 200 μs ($t_{off} = 0$ and $t_{on} = $ T) in our experiment.

The experimental setup scheme is shown in Fig. 2(a). Both the coupling and probe laser lights are issued from the same tunable external cavity diode laser of linewidth less than 1 MHz whose frequency could be tuned and stabilized along the Rb D_1 line (795 nm). The precise laser frequency position was monitored at an auxiliary saturated absorption setup. The 795 nm laser beam splits into two parts by the combination of half-wave plate and polarization beam splitter (PBS), where one serves as the probe light, and the other for the coupling one. An acousto-optical modulator (AOM) driven at 80 MHz provides an optical switching with a rise time around 100 ns for the coupling light. It is shown in Fig. 2(b). Another AOM is also driven at 80 MHz to provide frequency shift for the

probe light to achieve Raman resonance condition. After passing through the quarter-wave plate, the probe beam and the coupling light become left-handed and right-handed, respectively.

The sample cell is made of Pyrex glass, which is a 25-mm-diameter 100-mm-long Rb vapor cell. The cell contains a few milligrams of ^{87}Rb metal (isotopically enriched to an assay of 99.5%) and 8 torr of Ne. The buffer gas is more helpful to observe the fast transient optical process. A temperature control system with the accuracy of temperature to ± 0.05 °C is used to heat the cell at 50 °C. The cell is placed inside a cylindrical coil with a magnetic field applied along the laser propagation to define the quantum z-axis. A small magnetic field of 1 Gauss is enough for this purpose. The coil and the cell are placed inside a cylindrical μ-metal shield to reduce stray magnetic fields components along the cylindrical coil axis to less than 10 nT. The transient transmission signal of probe beam is detected by a fast photo detector.

As the coupling laser is right-polarized and its beam power (< 5 mW) is much stronger than that of the probe one (50 μW), the atom will accumulate on the state $|F = 2, m_F = 2\rangle$, showing an obvious polarization population. The coupling laser has a Rabi frequency Ω_c less than $2\pi \times 20$ MHz while the probe has Rabi frequency $\Omega_p \sim 2\pi \times 1$ MHz. This polarization process will also be discussed later.

3. Results and discussion

Experimentally, we firstly record the transient transmission spectrum of probe light in the ^{87}Rb Λ-system by turning on or off the coupling light beam sequentially. The spectra have been acquired under the condition that the coupling laser is tuned resonant to the transition $F = 2 \rightarrow F' = 2$ of ^{87}Rb D_1 line. We find that the temporal evolution profile of the Zeeman EIT probe light transmission signal is also related to the coupling light laser power and the Rb cell temperature. Unlike the research on pure transient spectral recording as in Refs. [25,26], we focus on the study of the Zeeman transverse relaxation dynamics. We build a time-dependent optical Bloch equation considering dephasing processes between Zeeman sublevels, which is helpful for understanding the concerned process better.

As is expected, the laser-atom system shows different transient dynamics when the coupling light is turned off and turned on. Its experimental observation is shown in Fig. 3, where the coupling laser is locked to the transition $F = 2 \rightarrow F' = 2$. We can see that all spectra at different coupling laser powers varying from 0.5 mW to 2.5 mW have similar structures responding to the coupling laser switching. As shown in Fig. 1, when the coupling laser is much stronger than the probe one, the atom is completely transferred onto state $|F = 2, m_F = 2\rangle$ and gets mostly σ^+ polarized. At this moment, a simplified steady EIT is formed via the energy levels $|F = 2, m_F = 0\rangle$, $|F' = 2, m'_F = 1\rangle$ and $|F = 2, m_F = 2\rangle$, and the probe light is highly transmitted across the atomic medium, as shown at $t < 0$ μs in Fig. 3.

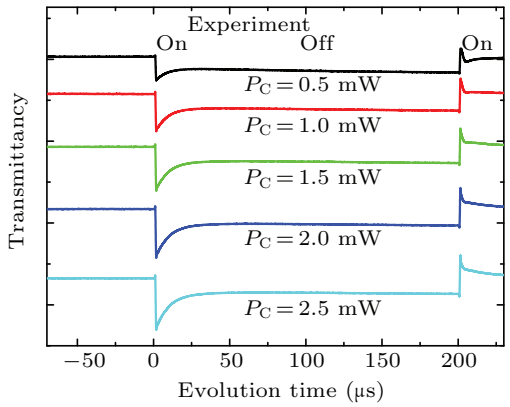


Fig. 3. Experimental observation of transient transmission spectra with the coupling light laser power varying from 0.5 mW to 2.5 mW at the coupling light tuned to transition $F = 2 \rightarrow F' = 2$. The coupling beam is turned off at zero time and turned on at later time $t = 200$ μs.

Just after the coupling laser is switched off, the atoms accumulated on state $|F = 2, m_F = 2\rangle$ will be depleted under the weak probe laser beam, showing a strong absorption, corresponding to a spectral dip at time of 0 μs as shown in Fig. 3. A small upward peak just before time zero is due to the electric reflection of the AOM switching driver although the applied magnetic field to define the quantum z-axis also serves to split the energy levels a little to shift the EIT spectral lines away from the beating signal between the probe and coupling lights. As the probe laser is σ^- polarized, the atom will be transferred towards another extreme $|F = 2, m_F = -2\rangle$. Under the single beam, the probe light, the atom suffers a cascading transferring from $|F = 2, m_F = 2\rangle$ and gets saturated very slowly since the probe laser is much weak. This conflicts with the observation where the rising occurs in ~ 1 μs. Even an equilibrium arrives, the atomic vapor is no longer so transparent as the case with the coupling beam on. We expect it is due to the fluorescence relaxation process along the pump and probe optical transitions between different magnetic quantum number states between $F = 2$ and $F' = 2$, described by the relaxation term $-\frac{i}{2}\gamma_D$, which also includes other equivalent processes. Similar dephasing relaxation is introduced by the term $-\frac{i}{2}\gamma_d$ to describe the decaying between the adjacent Zeeman levels of the low $F = 2$ states as well as those for the upper state $F' = 2$.

This conjecture is confirmed by numerical analysis after introducing the concerned relaxation processes into the optical Bloch equation (1). It is shown in Fig. 4. We can see that if the two kinds of relaxations are absent in the equation, i.e., $\gamma_D = 0$ and $\gamma_d = 0$, there is no absorption dip at zero time, as shown in Fig. 4(a). However, if a small value of $\gamma_D = 0.2$ MHz introduced in the calculation, the dip structure comes out. It

is displayed in Fig. 4(b), where we can see a little rising tendency from zero time. If we extract this local data out and fit it with a bi-exponential function, two time characters can be determined with one of them being ~ 4 μs while the other being much long (235 μs), well characterizing the experimental observation in previous paragraph.

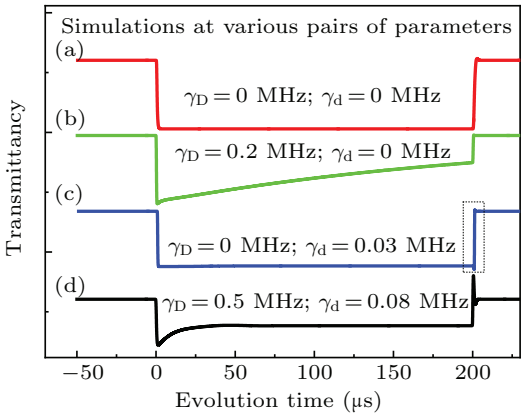


Fig. 4. Simulation of transient transmission spectrum for a long time evolution with coupling beam switching off and on. Two relaxation processes have been introduced into Eq. (1), characterized by γ_D and γ_d, (a) for the case without any relaxation process, (b) for the case with nonzero γ_D, (c) for nonzero γ_d, and (d) for both nonzero. The introduction of these two relaxation processes can well describe the main feature of the observation in Fig. 3. Note that the part in dotted line in (c) shows a low dip at 200 μs.

Now we turn to the second relaxation contribution characterized by γ_d. We set $\gamma_D = 0$ and apply a small value of $\gamma_d = 0.03$ MHz into the simulation. Its insertion does not contribute the dip structure but slightly modifies the fast transient dynamics at $t = 200$ μs. A very small dip forms, which recovers the fine structure of the experimental observation. Moreover, the peak just after the coupling beam switched on again is slightly weakened. The detail is presented in Fig. 4(c). The introduction of the relaxation term between Zeeman sublevels is a coherent term correlating the sublevels.[27] The population transfer occurs between these Zeeman sublevels.[28] If we replace the parameters to be $\gamma_D = 0.5$ MHz and $\gamma_d = 0.08$ MHz, we can notice that the dip at zero time is perfectly recovered, comparable to the experimental data, and the fast transient behavior can also be clearly seen. It is shown in Fig. 4(d). A better consistent simulation requires more tastes for better parameter values. The simulation helps us to attribute the main spectral characters to two different relaxation processes. Further studies show that the two interactions introduced are eventually correlated a little. Therefore, it is necessary to introduce the fluorescence relaxation term and the transverse decay term into the Lindblad term of the optical Bloch equation as described in Eq. (1). Only in this way, can we explain the fast sharp transmission at $t = 0$. This feature is neglected in previous studies.[25,26]

It should be noted that although we have applied the introduced γ_d and γ_D terms to all Zeeman states concerned in the transition $F = 2 \rightarrow F' = 2$ of ^{87}Rb D_1 line, involving the 5 Zeeman levels of the upper state $|F' = 2, m_{F'} = -2, -1, 0, 1, 2\rangle$ and 5 Zeeman levels of the lower state $|F = 2, m_F = -2, -1, 0, 1, 2\rangle$, the anisotropic features between different magnetic quantum number states are not individually considered. As described previously, they are simplified to two groups of parameters, γ_D and γ_d.

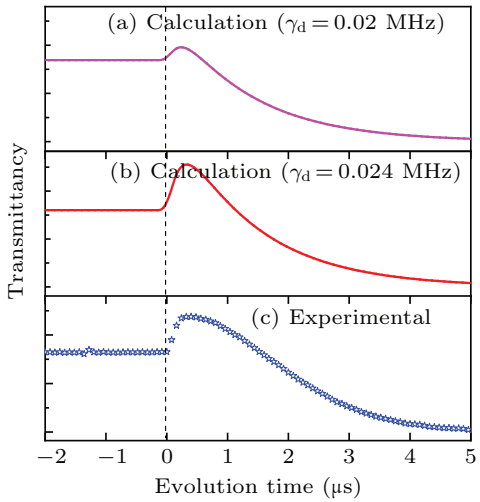


Fig. 5. The numerical matching just after coupling laser switching on at $t = 200$ μs [(a), (b)] for the fast transient spectrum (c), where the transverse relaxation time (T_2) can be determined. The zero has shifted to $t = 200$ μs.

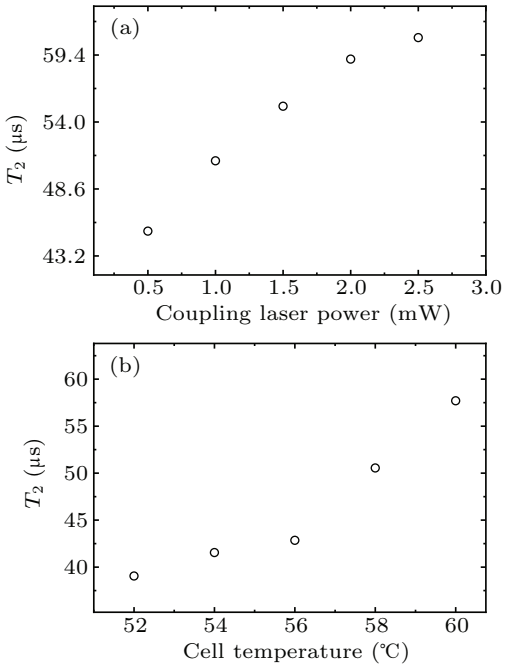


Fig. 6. The transverse relaxation time (T_2) dependence on coupling laser beam power (a) and on the cell temperature (b) at coupling light resonant to the transition $F = 2 \rightarrow F' = 2$. The transverse relaxation time is determined by matching the theoretical simulation with the experimental data as in Fig. 5.

We come to a conclusion that the unique transient spectral character can serve as an unambiguous method to determine the transverse decay process quantitatively, rather than the usual ones that extract the decaying information from the

spectral frequency shift.[11,24] Since the sharp transmission at $t = 200$ μs is mainly determined by γ_d in the numerical test, we can extract this local data out and take it to character the transverse dynamics. A typical simulation for matching the experimental observation is given in Fig. 5. Therefore, the transverse relaxation time (T_2) can be determined.

By supervising this small variation of the transient spectrum, we can find a monotone decreasing dependence of transverse relaxation time on the applied coupling beam power and cell temperature for the coupling light tuned to transition $F = 2 \rightarrow F' = 2$, as shown in Figs. 6(a) and 6(b), respectively, implying a sensitive change for the relaxation process due to atom-atom and atom-wall collisions.

This relaxation time dependence on temperature is also consistent with the measurement by detecting the frequency shifts due to the spin-exchange interaction[11] although their relaxation is defined between two hyperfine manifolds of the ground states while ours between the Zeeman sub-levels of one hyperfine state. A higher temperature can enhance the pressure thus increasing the transverse relaxation time below 20 torr for buffer gas Ne.[29] The pump laser can also be identically viewed with the temperature increasing due to heating effect. To reduce the chance of the atom colliding with the cell wall and then narrowing the spectral linewidth, usually some buffer gas has been filled in the cell.

This method is similar to the measurements of transverse relaxation times of aligned mercury atoms in the metastable 6^3P_2 state.[30] There a short gated strong RF pulse acts on the atomic metastable state and causes the depolarization equilibrium between the Zeeman sublevels. After pulse switching off the polarization restores again characterized by the transverse decay time. The transverse relaxation time is in order of a few tens of μs. In our work, we firstly polarize the atoms by a σ^+–σ^- EIT process and then keep the pump beam off for a time of 200 μs. After that, we observe the build-up process between Zeeman sublevels. The determined time is of several tens of μs for ^{87}Rb, which is in the same order of the intrinsic relaxation time of Cs for a magnetometer.[31,32] Many factors can account for the small values. In our case, the relaxation occurs under the illumination of the probe beam in the whole evolution process, which accelerates the depolarization of the ground state by dumping transition from the upper Zeeman sub-states. Another factor for the short relaxation time is the insignificant buffer gas pressure (8 torr) used in our case, which cannot block atoms from collision with the cell via viscosity.[33] Our results are also in the same order of the demonstration measurements of ^{87}Rb transverse relaxation in the study of relaxation measurement metrology.[34]

As detailed in the previous section, a small magnetic field of less than 1 Gauss is very necessary to define the quantum z-axis. Its application will not change the transient process since the Zeeman effect at low magnetic field is linear[35] and the effect due to the magnetic field is only observable or seems sensitive in high precision magnetometer.[36,37]

4. Conclusion

In summary, we present an alternative way to obtain the Zeeman transverse relaxation time of ^{87}Rb vapors with buffer gas by using the transient transmitted spectra versus probe light detuning by turning on and off the coupling one in a typical EIT Λ resonance system. The spectra depending on the coupling light laser power and vapor temperature have been studied at the coupling light tuned to transition $F = 2 \rightarrow F' = 2$ of ^{87}Rb D_1 line. At the same time, a theoretical simulation based on the time-dependent optical Bloch equation has also been performed to account for the observation and extract the corresponding Zeeman transverse relaxation time.

This could be a new way to investigate the interaction between the alkali metals and noble gases. Our technique is useful for studying vapor cell characterization of coherent population trap based atomic clocks and atomic magnetometer along the vapor temperature and laser beam power applied.

Acknowledgement

Project supported by the National Natural Science Foundation of China (Grant Nos. 12074388 and 12004393).

References

[1] Seltzer S J, Rampulla D M, Rivillon-Amy S, Chabal Y J, Bernasek S L and Romalis M V 2008 *J. Appl. Phys.* **104** 103116
[2] Julsgaard B, Sherson J, Cirac J I, Fiurasek J and Polzik E S 2004 *Nature* **432** 482
[3] Kuzmich A, Mandel L and Bigelow N P 2000 *Phys. Rev. Lett.* **85** 1594
[4] Zhao S C, Wu Q X and Ma K 2016 *Chin. J. Phys.* **54** 756
[5] Zhang H, Zou S, Chen X Y and Li Y 2015 *J. Korean Phys. Soc.* **66** 1212
[6] Budker D and Romalis M 2007 *Nat. Phys.* **3** 227
[7] Seltzer S J and Romalis M V 2009 *J. Appl. Phys.* **106** 114905
[8] Brandt S, Nagel A, Wynands R and Meschede D 1997 *Phys. Rev. A* **56** R1063
[9] Katsoprinakis G E, Dellis A T and Kominis I K 2007 *Phys. Rev. A* **75** 042502
[10] Dreiling J M, Norrgard E B, Tupa D and Gay T J 2012 *Phys. Rev. A* **86** 053416
[11] Liu X H, Luo H, Qu T L, Yang K Y and Ding Z C 2015 *AIP Adv.* **5** 107119
[12] Khalkhali S M H, Ranjbaran M, Mofidi D, Hamidi S M and Tehranchi M M 2017 *Chin. J. Phys.* **55** 301
[13] Horsley A, Du G X, Pellaton M, Affolderbach C, Mileti G and Treutlein P 2013 *Phys. Rev. A* **88** 063407
[14] Jeong H and Du S W 2009 *Phys. Rev. A* **79** 011802
[15] Jeong H and Du S 2010 *Opt. Lett.* **35** 124
[16] Wei D, Chen J F, Loy M M T, Wong G K L and Du S 2009 *Phys. Rev. Lett.* **103** 093602
[17] Jeong H and Du S 2010 *Opt. Lett.* **35** 124
[18] Meinert F, Basler C, Lambrecht A, Welte S and Helm H 2012 *Phys. Rev. A* **85** 013820
[19] Shwa D and Katz N 2014 *Phys. Rev. A* **90** 023858
[20] Meinert F, Basler C, Lambrecht A, Welte S and Helm H 2012 *Phys. Rev. A* **85** 013820
[21] Valente P, Failache H and Lezama A 2003 *Phys. Rev. A* **67** 013806
[22] Li Y Q and Xiao M 1995 *Opt. Lett.* **20** 1489

[23] Shuker M, Firstenberg O, Sagi Y, Ben-kish A, Davidson N and Ron A 2008 *Phys. Rev. A* **78** 063818
[24] Corsini E P, Karaulanov T, Balabas M and Budker D 2013 *Phys. Rev. A* **87** 022901
[25] Chen H X, Durrant A V, Marangos J P and Vaccaro J A 1998 *Phys. Rev. A* **58** 1545
[26] Greentree A D, Smith T B, de Echaniz S R, Durrant A V, Marangos J P, Segal D M and Vaccaro J A 2002 *Phys. Rev. A* **65** 053802
[27] Tan W H and Zhang W P 1985 *Chin. Phys. Lett.* **2** 309
[28] Ke H L, Miao P X, Yang S Y, Tu J H, Hao J, Zhu L L, Yang B, Wang J, Yang W, Cui J Z and Sun R T 2019 *Optik* **180** 517
[29] Minemoto T and Kanda T 1971 *J. Phys. Soc. Jpn.* **31** 1174
[30] Jacobson E 1977 *J. Phys. B* **10** 3409
[31] Fu Y Y and Yuan J 2019 *Chin. Phys. B* **28** 098504
[32] Liu X J, Ding M, Li Y, Hu Y H, Jin W and Fang J C 2018 *Chin. Phys. B* **27** 073201
[33] Luo J, Wu Z H, Zhao M X, Chen A Q and Zeng X Z 1996 *J. Phys. B* **29** 3319
[34] Ding Z, Yuan J, Li Y, Feng W and Wang Z 2015 *Acta Opt. Sin.* **35** 0602002 (in Chinese)
[35] Sarkisyan D G, Papoyan A V, Varzhapetyan T S, Blush K and Auzinsh M 2014 *Opt. Spectrosc.* **96** 328
[36] Horsley A, Du G X, Pellaton M, Affolderbach C, Mileti G and Treutlein P 2013 *Phys. Rev. A* **88** 063407
[37] Li Q, Zeng X, Zhang J *et al.* 2011 *Academic International Symposium on Optoelectronics and Microelectronics Technology*, October 12–16, 2011, Harbin, China, pp. 27–30